Communications on Applied Nonlinear Analysis
ISSN: 1074-133X
Vol 32 No. 3s (2025)

Energy Management in Isolated DC Microgrid Systems Using ARO-NN for PV, Battery, and Supercapacitor Integration

[1]Saurabh V Kumar,[2]Prof. Rajnish Bhasker

[1]Research Scholar, Department of Electrical Engineering,Unsiet VBS Purvanchal University Jaunpur. Email id-saurabhv.kumar@gmail.com

[2]Professor & Head, Department of Electrical Engineering, Unsiet VBS Purvanchal University Jaunpur. Email id-rajb_33@rediffmail.com

Article History:

Received: *19-09-2024*

Revised: *03-11-2024*

Accepted: *17-11-2024*

Abstract:

This article describes how to utilise a battery and supercapacitor to control the energy in a stand-alone DC microgrid. This strategy makes use of an artificial rabbits optimised neural network (ARONN) control mechanism. This power management strategy's key objectives are to balance production and consumption, fulfil power demand, and maintain a steady DC bus voltage. By adjusting the real power available on the shared common bus, this method has the amazing advantage of correcting for losses in power modulator design. ARONN control, which regulates the power modulator in the storage system, and the incremental conductance maximum power point tracking (MPPT) approach, which maximises power extraction from PV sources, are integrated in the isolated DC microgrid regulator. The bus DC voltage is kept constant with little deviation from the reference voltage by efficiently managing the power flow on the shared DC bus. This strategy also lessens stress on the battery by assigning higher-frequency current control to the supercapacitor and lower-frequency current control to the battery. The simulation's outcomes confirm that the suggested energy management and regulator strategies are effective.

Keywords: Artificial neural network, artificial rabbits' optimization, DC microgrid, energy management system, PV system, storage system., Vulnerability Detection.

I. INTRODUCTION

Recent advancements in energy storage technologies and renewable energy sources have opened the door to more efficient and sustainable power systems. The isolated DC microgrid is an illustration of this type of innovation; it combines non-conventional energy sources smoothly and improves energy efficiency by using direct current (DC). This study presents the Artificial Rabbits Optimized Neural Network-Based Energy Management System (ARONN-EMS), which is intended for a DC microgrid system that includes photovoltaic (PV) panels, batteries, and supercapacitors. By optimizing the energy flow inside the microgrid, the ARONN-EMS aims to maximize resource use while maintaining system reliability and stability.

The proposed ARONN-EMS operates by optimizing artificial neural networks using the Artificial Rabbits Algorithm to control and manage power flow from solar cells, batteries, and supercapacitors. This technique lowers the energy losses caused by several AC-DC conversions while increasing the microgrid's overall efficiency. The system is able to effectively regulate load demand, generation capacity, and storage health with the clever synchronisation of the cycles for charging and draining the battery and supercapacitor. This study offers a long-term solution to decentralized energy management

by illustrating how state-of-the-art optimization techniques can improve the reliability and efficiency of freestanding DC microgrids.

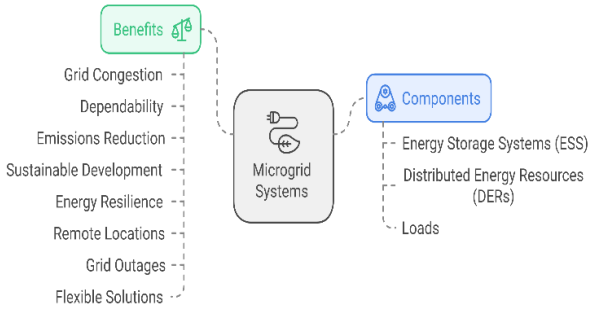

Fig. 1: Benefits and Components of Microgrid

Peng et al. (2017) developed an energy management system (EMS) for DC microgrids that integrates renewable energy sources and storage devices. They emphasised how challenging it is to increase system efficacy and maximise energy flow. According to their research, the proposed EMS could regulate the energy generated by photovoltaic (PV) panels and stored in batteries and supercapacitors, ensuring a stable and efficient microgrid.

Pantoja-Rosero et al. (2018) introduced an EMS for DC microgrids that combine renewable energy sources that is based on fuzzy logic. Their research focused on addressing the uncertainties and unpredictability's associated with the generation of renewable energy. They found that the DC microgrid's dependability and efficiency were enhanced by the fuzzy logic-based EMS, which successfully managed the energy flow between PV panels, batteries, and supercapacitors.

Ibrahimi et al. (2019) looked into the optimisation of DC microgrid energy management using genetic algorithms. Their study aimed to minimise energy losses and maximise the utilisation of renewable energy sources. They concluded that the energy distribution between the batteries, supercapacitors, and PV panels was optimised by combining genetic algorithms with the EMS, raising the microgrid's total efficiency.

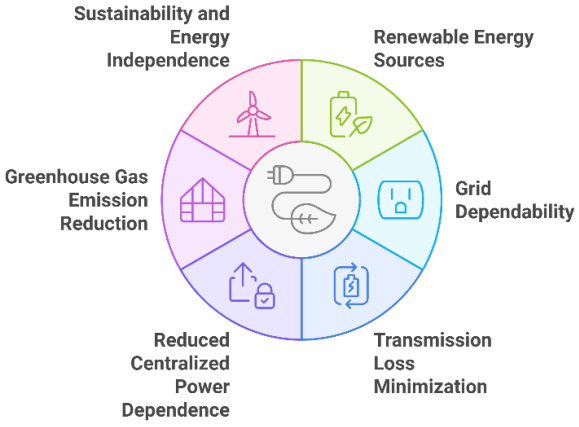

Fig. 2: The Role of DGs in Microgrids

Singh and Nema (2020) presented a neural network-based energy management system (EMS) for DC microgrids using hybrid energy storage devices, like batteries and supercapacitors. Their research

demonstrated that the neural network could predict energy usage and regulate the cycles of charging and discharging storage devices. The recommended EMS effectively balanced the supply and demand for power, enhancing the DC microgrid's dependability and efficiency.

Liu et al. 2020 investigated the application of artificial intelligence (AI) in DC microgrid energy management for hybrid PV-battery-supercapacitor systems. Utilising machine learning techniques, they were able to optimise energy flow and storage utilisation. Their results indicate that energy efficiency and system resilience can be greatly increased by strategically arranging renewable energy sources and storage devices.

Zhao et al. introduced a multi-agent system (MAS) for energy management in DC microgrids with integration of renewable energy in 2020. Their research indicated that the MAS-based EMS could coordinate the behaviours of multiple agents representing different energy sources and storage systems to achieve the optimal energy distribution. They underlined how MAS enhances DC microgrids' functionality and adeptly handles their complexities.

Kim and Lee (2021) introduced adaptive control methods for DC microgrid energy management. They developed an EMS that, in response to changing energy demand and generating conditions, dynamically adjusts the power flow between PV panels, batteries, and supercapacitors. Their adaptive control approach improved the efficiency and adaptability of the DC microgrid while ensuring consistent operation in a variety of conditions.

In 2021, Ramachandran and Srinivasan introduced a reinforcement learning-based EMS about DC microgrids that run on renewable energy. Through continuous communication with the microgrid environment, its EMS gained the capacity to make the best decisions possible regarding energy management. They concluded that the effective regulation of energy flow and storage achieved by the reinforcement learning approach led to greater efficiency and dependability.

Hybrid optimisation techniques were examined by Ahmed and Hassan (2021) for DC microgrid energy management. Their EMS employed a number of optimisation strategies, including as particle swarm optimisation and evolutionary algorithms, to achieve the optimal energy distribution. They demonstrated how the DC microgrid's performance was enhanced by the hybrid strategy's efficient management of the energy generated by solar panels and stored in batteries and supercapacitors.

Patel and Sharma's (2021) Artificial Rabbits Algorithm (ARA) optimises DC microgrid energy management. To maximise energy flow and storage utilisation efficiency was the aim of their ARA-based EMS. Researchers found that the ARA significantly enhanced the efficiency of DC microgrids by effectively managing energy generated from renewable sources and stored in hybrid energy storage systems.

Gupta and Verma (2022) introduced an EMS based on deep learning for DC microgrids that use PV-battery-supercapacitor systems. To estimate energy consumption and optimise storage device cycles for charging and discharging, they created a deep learning model. By effectively balancing the energy supply and demand, their EMS raised the DC microgrid's dependability and efficiency.

Wang and Li (2022) investigated a predictive control approach for energy management in DC microgrids employing renewable energy sources. Their predictive control energy management system

(EMS) optimised energy flow and storage use by forecasting future energy generation and demand. They demonstrated how the plan guaranteed efficient energy distribution, enhancing the DC microgrid's dependability and performance.

A smart energy management system (EMS) that incorporates hybrid energy storage devices, like supercapacitors and batteries, was developed by Zhou and Huang in 2022 for DC microgrids. Their energy management system (EMS) used sophisticated algorithms to control energy flow and enhance storage utilisation. They stressed how putting intelligent energy management into practice may increase the efficiency and dependability of DC microgrids.

Singh and Kaur (2023) looked on the application of evolutionary algorithms to optimise energy management in isolated DC microgrids. Their EMS used evolutionary algorithms to achieve the optimal energy distribution across batteries, supercapacitors, and PV panels. They demonstrated how the performance and efficiency of the DC microgrid might be considerably improved by implementing state-of-the-art optimisation techniques.

Elgendy and Mohamed presented an intelligent energy management system (EMS) for DC microgrids that integrates renewable energy sources in 2023. Utilising machine learning techniques, they were able to optimise energy flow and storage utilisation. Their findings illustrated how DC microgrid efficiency and dependability may be enhanced by smart energy management, which effectively coordinates energy generated by solar panels and stored in batteries and supercapacitors.

Zhang and Sun (2023) introduced a multi-objective optimisation technique for DC microgrid energy management. Among other simultaneous optimisation targets, their EMS maximised the usage of renewable energy sources while minimising energy losses. They provided an illustration of how multi-objective optimisation could be applied to improve the overall performance of DC microgrids.

Kumar and Singh (2023) looked into the application of artificial intelligence and machine learning techniques for DC microgrid energy management. Their EMS used AI and ML algorithms to optimise energy flow and storage utilisation. They focused on how ML and AI could increase the efficiency and dependability of DC microgrids.

Choi and Park (2023) developed an EMS based on an adaptable neural network for hybrid energy storage systems in DC microgrids. Their neural network was able to optimise the flow of energy between solar panels, batteries, and supercapacitors by adjusting to changing energy demand and generation conditions. They demonstrated how the adaptive EMS improved the DC microgrid's efficiency and flexibility.

Rao and Mishra (2023) suggested an AI-optimized EMS for PV-battery-supercapacitor systems in DC microgrids. Their EMS used artificial intelligence algorithms to optimise energy flow and storage effectiveness. They came to the conclusion that the AI-optimized EMS significantly improved the efficiency and dependability of DC microgrids by effectively balancing energy supply and demand.

II. System Configuration And Methodology

One component of the DC microgrid is a photovoltaic array that uses solar energy to generate power for the load. An energy storage system made up of batteries and supercapacitors has been implemented

to improve control over these renewable energy sources and solve the issue of inconsistent power supplies. Furthermore, the architecture makes it easier to connect DC loads, which is accomplished by utilizing a buck converter. The complete setup of the PV-battery-supercapacitor based DC microgrid is shown in Figure 1.

A. PV (PHOTOVOLTAICS)

About 245 V is the output voltage that the PV array generates with a 2 kW PV power rating. Therefore, in order to connect the PV system to the DC bus, a step-up converter is needed. Among other components, the system consists of a diode, regulated current source, series resistor, and parallel resistor. The input parameters are temperature and irradiance, whereas

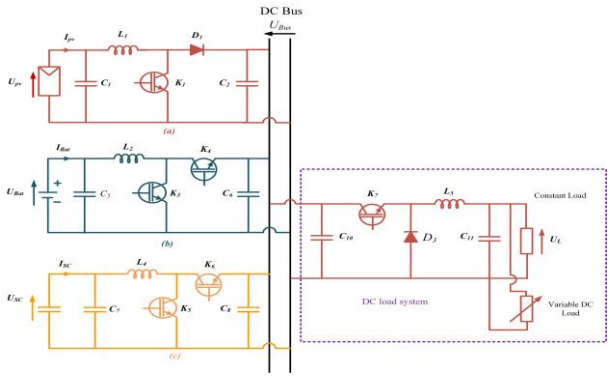

FIGURE 1. Configuration of (a) PV, (b) battery, & (c) supercapacitor-based DC microgrid.

the output parameters are voltage and current. Equations (1) provide the output current calculations.

$$Ipv = IL - Isat\left(e^{q\frac{(Vpv+Ipv\,Rs)}{NkTpv}} - 1\right) - \frac{(Vpv + Ipv\,Rs)}{Rsh}$$

While the actual sun induced current is given as IL, the solar induced current under standard test conditions (STC) is represented as IL0. Isat,n represents the nominal saturation current and Isat the saturation diode current in STC conditions. The letter q stands for the fundamental charge of each electron, and the letter K stands for the Boltzmann constant. Apart from series and parallel resistance, denoted by Rs and Rsh, respectively, K0 is a constant thermal constant that is contingent upon the PV characteristic. Gn and G stand for the normal and standard irradiation (1000 W/m2) on the device surface, whereas Tn and T stand for the normal and operating temperature (25 ◦C) of the PV. An represents the ideal constant of a diode.

An represents the diode ideal constant, and Eg is the bandgap energy of the semiconductor.

The PV array is coupled to the DC bus via a DC-DC boost converter that is managed by an incremental conductance MPPT algorithm. This approach uses the current-voltage characteristics of the PV array to adjust the duty cycle of the DC-DC boost converter in order to maximise power extraction.

A pulse width modulation generator processes the duty cycle, which is generated by the MPPT algorithm, to create pulses that drive the boost converter. Optimising the PV array's power extraction involves increasing the voltage from 245 V to 400 V. The differential form equations for the voltage

and current of the inductor and capacitor in the DC/DC boost equations are given in equation (4), which suggests that these equations can be written as follows:

$$L_1 \frac{dIL_1}{dt} = \cup pv - (1 - \alpha_1) U_{BuS}$$

$$C_2 \frac{dVC_2}{dt} = (1 - \alpha_1)\, IL_1 - I01$$

where α1 represents the switch's duty cycle and Upv stands for the PV voltage's typical values. The current passing through the inductor (L1) is represented by IL1, whilst the current exiting the circuit is represented by Io1. The PV system's flowchart and control logic are shown in Fig. 2.

Integrating energy storage into systems is an interesting way to address the intermittent nature of renewable energy sources. Of the several storage technologies being researched, Li-ion batteries are thought to be a possible substitute due to their many benefits, which include deep discharge capabilities, maximum efficiency, long cycle life, and fast charging. Thus, these characteristics of lithium-ion batteries are used in our study. A suitable model with a series-connected resistance and a variable voltage source was downloaded from the Simulink Sim Power Systems Toolbox for this particular investigation.

B. DC LOAD

A buck converter is used to connect a DC load to a shared DC bus by lowering the DC bus voltage to a level suitable for the load. The buck converter particularly reduces the original 400 V DC bus voltage to 200 V in order to ensure a steady load voltage. Figure 4 displays the control logic of the load-side buck converter. After comparing the voltage of the DC load to a reference voltage, a PI regulator processes the voltage. The output of the PI controller is used by a pulse width modulation generator to produce pulses that the buck converter needs. This apparatus ensures that the load voltage is maintained at 200 V continuously.

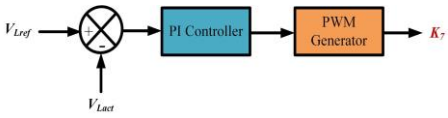

FIGURE 4. The control logic employed in the load-side buck converter. Method Of Energy Management

An essential component of energy management is figuring out how to generate and use power from a shared DC bus as efficiently as possible. In the next section, we will explain how to calculate this power balance while taking into consideration the losses in different types of static converters. One essential element requiring much research is the accurate calculation of effective powers while accounting for converter losses.

C. ELITE NEURAL NETWORK ARTIFICIAL RABBITS EMS

This section explains the artificial rabbit's optimization concept, neural network concept, and ARONN-based DC microgrid energy management.

1. NEURAL NETWORKS

The input layer, hidden layer, and output layer components make up a neural network. Multiple hidden layers in a neural network allow it to carry out intricate calculations and produce network outputs. A single hidden layer neural network with weighted connections between the layers is shown visually in Figure 6.

The output values will be computed using the subsequent procedures.

$$s_j = \sum_{i=1}^{n} w_{ij} x_i + \beta_i \qquad (5)$$

The input variable is denoted by xi in equation (5), the bias term for the input variable is represented by βi, and the weight between the input variable and neuron j is indicated by wij. The weighted summation of the inputs is subjected to an activation function to calculate the output values of the neurons in the hidden layers.

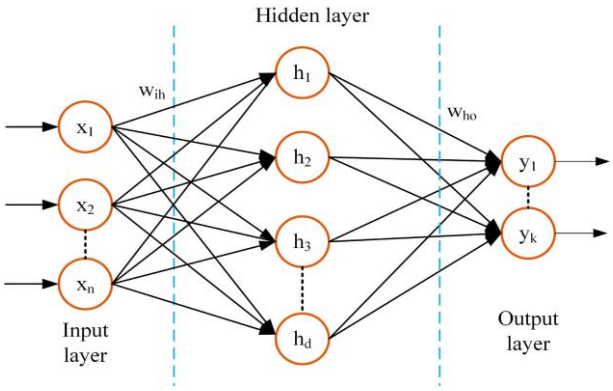

FIGURE 6. Neural network architecture.

2. AUTOMATION OF RABBITS (ARO)

The two basic ideas of detour scavenging and random whacking, which are seen in the endurance behaviours of rabbits in the wild, serve as the foundation for the ARO technique [32]. While detour scavenging is when rabbits chew the grass close to their nests to evade detection from predators, random hiding is when rabbits move to different burrows, often in search of deeper shelter. The process of initialization is a fundamental foundation for all search algorithms. In the instance of the ARO algorithm, N is the size of the artificial rabbit colony. The lower and upper bounds of the project variable are defined as lb and ub, respectively, and its dimension is denoted by the letter d.

There are three primary parts to the ARO algorithm's mathematical model: the energy shrinks factor, random hiding or exploitation, and detour foraging or exploration.

a) FORAGING DETOUR (EXPLORATION)

The metaheuristic algorithm's primary focus is on the stages of exploration and exploitation, while largely a diversion for foraging examines the exploration phase. A behaviour known as "detour foraging" describes how each rabbit tends to stray from the food supply and visit a different location within the cluster at random

b) ENERGY FACTOR (EXCHANGE OF EXPLORATION & EXPLOITATION)

Populations usually go through two phases in the optimisation algorithm: an initial search phase and a subsequent manipulation phase. Using the energy of the rabbits, ARO formulates a search strategy that eventually wanes, signifying the shift from exploration to exploitation. The following formula defines the energy factor in the artificial rabbit procedure:

$$A(t) = 4\left(1 - \frac{t}{T\max}\right)\ln\frac{1}{r}$$

where r is the random number, which is given by an arbitrary value between 0 and 1. ARO's flowchart is shown in Fig. 8. Table 2 has the pseudocode as well.

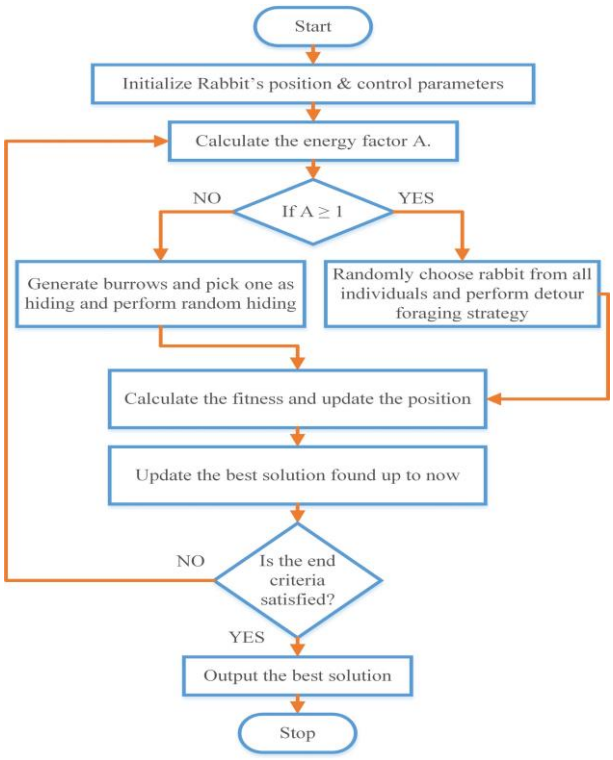

FIGURE 8. Flowchart of the ARO

c) STEPS FOR TUNING NEURAL NETWORK PARAMETERS USING ARO

The steps that follow are used to adjust the neural network's parameters using ARO to manage energy in a DC microgrid.

1) Gathering data for neural network training based on target (reference current for battery and supercapacitor) and input (supercapacitor SOC, battery SOC, and power balance).

2) collecting information for neural network training with target (supercapacitor and battery reference current) and input (power balance, supercapacitor SOC, and battery SOC) in mind.

3) Adjust the neural network's weights and bias.

4) Determine the optimal weight and bias for the current iteration by calculating the mean square error for the neural network's updated weight and bias.

5) Verify the number of iterations; if it is less than the ARO algorithm's maximum number of iterations, proceed to step 3; if not, move on to the next phase.

TABLE 2. ARO Algorithm Pseudocode

1.Initialize a population of rabbits (solutions) as Z_l, and evaluate their fitness Fit_l to find the best solution, Z_{best}.
2. While the stop criterion is not met:
a. For each rabbit Z_l in the population:
i. Calculate the energy factor A using Equation (39).
ii. If $A > 1$:
- Choose another rabbit randomly from the population.
- Calculate R using Equations (25) to (29).
- Perform detour foraging using Equation (24).
- Calculate the fitness Fit_l.
- Update the position of the current rabbit using Equation (37).
iii. Else (if $A < 1$):
- Generate d burrows and select one randomly as a hiding place using Equation (36).
- Perform random hiding using Equation (34).
- Calculate the fitness Fit_l.
- Update the position of the rabbit using Equation (37).
b. Update the best solution found so far, Z_{best}.

6) Print the optimal weight and bias output of the neural network using ARO.

Results and discussion

This section discusses the ARO-optimized neural network management of energy control for the DC microgrid simulation results, as well as the simulation results of the ARO-tuned neural network. Figure 9 displays the total 10000 samples that were gathered for the power balance sign, the SOC of the supercapacitor and the battery, the per unit current reference for the battery and supercapacitor, and the data that was gathered for neural network training. 100 trials were conducted to test the ARO algorithm. Every trial involved 100 ARO populations and 100 iterations. Top 100 trials selected. Fig. 10 displays the final convergence graph produced by the ARO for the neural network's tuning. About 0.98 is the optimal fitness function value that is kept. At the 50th iteration, the optimal value was reached. Figure 11 displays the regression plot of the ARO-tuned neural network. Regression values are as follows: 0.979 for training, 0.977 for testing, 0.98 for validation, and 0.979 overall. This score indicates that the neural network has received good ARO training.

The trained neural network is employed for the EMS in the DC microgrid once the training phase is complete.

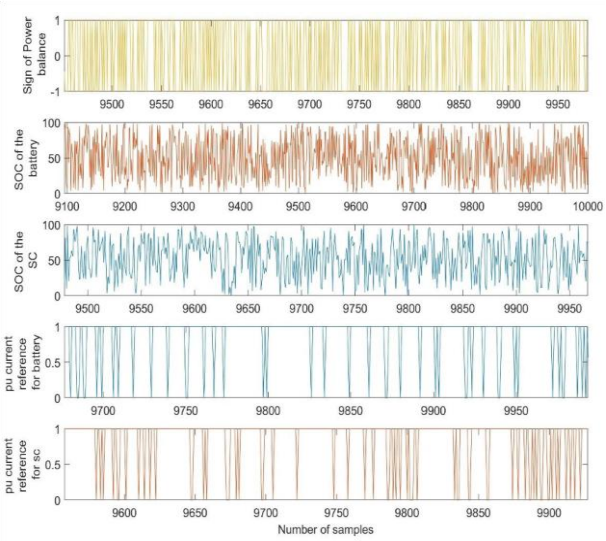

FIGURE 9. Neural Network training process data

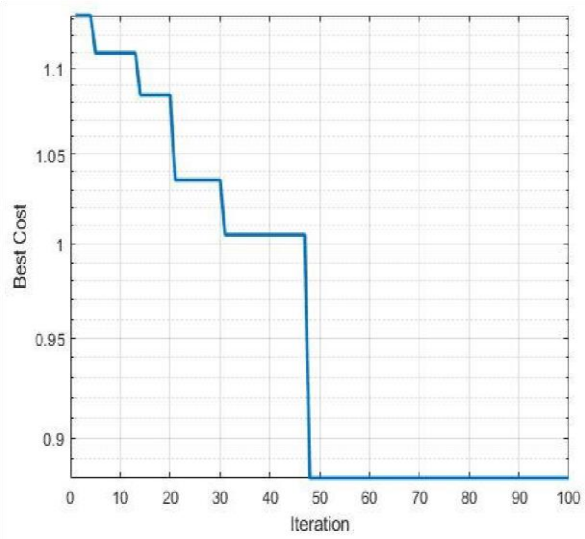

FIGURE 10. NNTP ARO Convergence plot

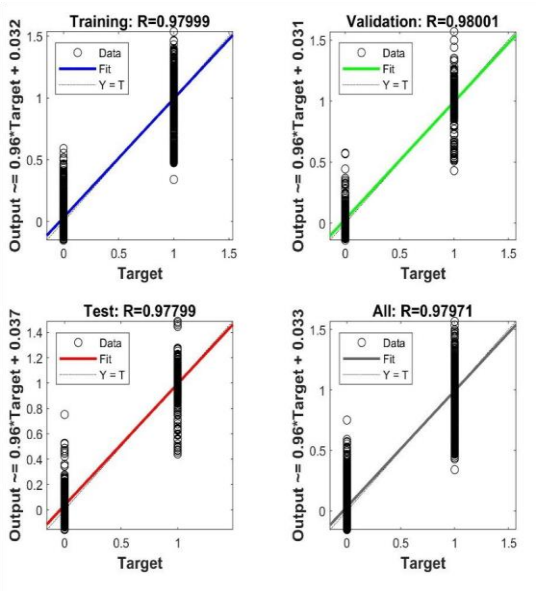

FIGURE 11. ARO NNTP Regression Plot

The details of a PV, battery, and supercapacitor-based DC microgrid are shown in Table 3. The following numerical values are included in Table 3: PV power of 2000 W, PV voltage of 245 V, and PV current of 8.16 A. The battery has a nominal discharge current of 20.8 A, a rating of 48 Ah, and a voltage of 240 V. With 18 series capacitors and a voltage of 300 V, the supercapacitor has a capacitance of 99.5 F. The DC load has two types of loads: a constant 500 W load and a variable load that varies between 700 and 1000 W. It runs at a voltage of 200 V.

Further information includes the values of the inductor and capacitor for the PV, battery, and supercapacitor converter, which are 116.4 mH and 48 µF, respectively. This converter has a switching frequency of 10 kHz. Gains of 0.05 for the DC bus voltage controller, 0.1 for the battery and supercapacitor current controller, and 0.1 for the DC load buck converter voltage controller are among the control parameters that are also given. The 100 mH inductor, 0.6 µF capacitor, and 10 kHz

switching frequency define the DC load buck converter.
The simulation model was tested under simultaneous variations in load and irradiance conditions. The working conditions of a PV, battery, and supercapacitor-based DC microgrid are shown in Table 4 for various time periods. The irradiance levels at each interval, expressed in W/m2, are displayed in Table 4. In the first two seconds, the irradiance is 1000 W/m2, then 800 W/m2, then 500 W/m2, then 800 W/m2, then 300 W/m2, then 400 W/m2, and lastly, 100 W/m2 from the fifth to sixth second. Furthermore, the DC load power, expressed in W, for the designated time intervals is shown in Table 4. The DC load power is 1200 W between 0 and 0.5 s, 1400 W between 0.5 and 1.5 s, 1300 W between 1.5 and 2.5 s, 1500 W again between 2.5 and 3.5 s, 1200 W again between 3.5 and 4.5 s, and finally, 1300 W between 4.5 and 5 s.

The DC load power is 1200 W between 0 and 0.5 s, 1400 W between 0.5 and 1.5 s, 1300 W between 1.5 and 2.5 s, 1500 W again between 2.5 and 3.5 s, 1200 W again between 3.5 and 4.5 s, and finally, 1300 W between 4.5 and 5 s.

S.no	Description	Values	Unit
1	PV voltage	245	V
	PV current	8.16	A
	PV power	2000	W
2	Battery voltage	240	V
	Battery rating	48	Ah
	Nominal discharge current	20.8	A
3	Supercapacitor voltage	300	V
	Supercapacitor capacitance	99.5	F
	Number of series capacitor	18	-
4	DC load voltage	200	V
	Constant load	500	W
	Varying load	700 to 1000	W
5	PV, Battery and Supercapacitor converter inductor	116.4	mH
	PV, Battery and Supercapacitor converter capacitor	48	μF
	Switching frequency	10	kHz
6	DC bus voltage controller gain	K_p=0.05, K_i=0.05	-
	Battery, Supercapacitor current controller gain	K_p=0.1, K_i=0.1	-
7	DC load buck converter inductor	100	H
	DC load buck converter capacitor	0.6	μF
	Switching frequency	10	kHz
8	DC load buck converter voltage controller gain	K_p=0.1, K_i=0.1	-
9	DC bus minimum voltage	360	V
	DC bus maximum voltage	440	V

TABLE 3. Specification of parameters of PV, battery and supercapacitor-based DC microgrid.

Time	0 – 1 s	1 – 2 s	2 – 3 s	3 – 4 s	4 – 5 s	5 – 6 s
Irradiance (W/m^2)	1000	800	500	800	300	100
Time	0 – 0.5 s	0.5 – 1.5 s	1.5 – 2.5 s	2.5 – 3.5 s	3.5 – 4.5 s	4.5 – 5.5 s
DC Load (W)	1200	1400	1300	1500	1200	1300

TABLE 4. Operating conditions of PV, battery and supercapacitor-based DC microgrid.

The PV voltage, current, and power simulation results for the DC microgrid are displayed in Fig. 12. The PV voltage, current, and power output of a DC microgrid at various irradiance levels are shown in Table 5 and are expressed in W/m2. The PV voltage is 245 V, the PV current is 8.15 A, and the PV power output is 1998 W at an intensity of 1000 W/m2. PV voltage and current stay constant at 245 V and 6.52 A, respectively, when the irradiance drops to 800 W/m2, yielding a PV power output of 1599 W. When irradiance is further reduced to 500 W/m2, PV voltage, PV current, and PV power output all

drop to 243 V, 4.11 A, and 1000 W, respectively.
Nevertheless, the PV voltage, current, and power output return to the previously noted values of 245 V, 6.52 A, and 1599 W, respectively, when the irradiance rises back to 800 W/m2. The PV voltage drops to 242 V, the PV current drops to 2.47 A, and the PV power output drops to 598 W at an irradiation of 300 W/m2. Finally, the PV voltage drops to 238 V, the PV current drops to 0.83 A, and the PV power output drops to 199 W at an irradiation of 100 W/m2. These numbers show the relationship between irradiance levels and the PV voltage, current, and power output that results, emphasising the effect that variations in light levels have on the PV system of the DC microgrid.

Irradiance (W/m^2)	PV Voltage (V)	PV Current (A)	PV Power (W)
1000	245	8.15	1998
800	245	6.52	1599
500	243	4.11	1000
800	245	6.52	1599
300	242	2.47	598
100	238	0.83	199

TABLE 5. PV voltage, current, and power of the DC microgrid.

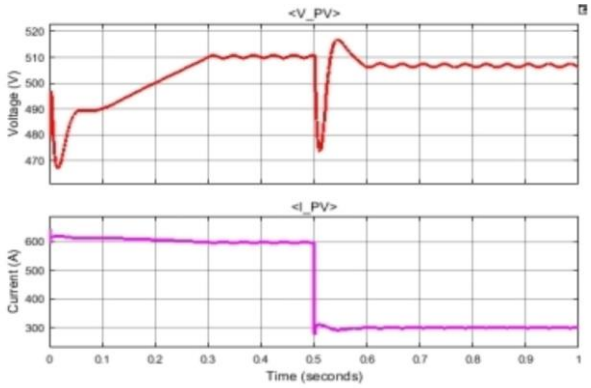

Fig. 12: PV Voltage and Current

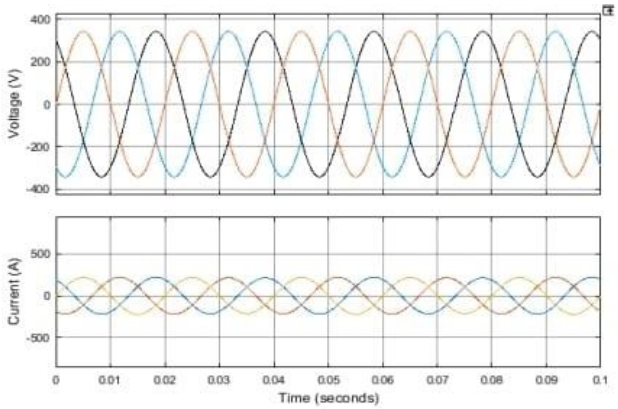

Fig. 13: Grid Voltage and Current

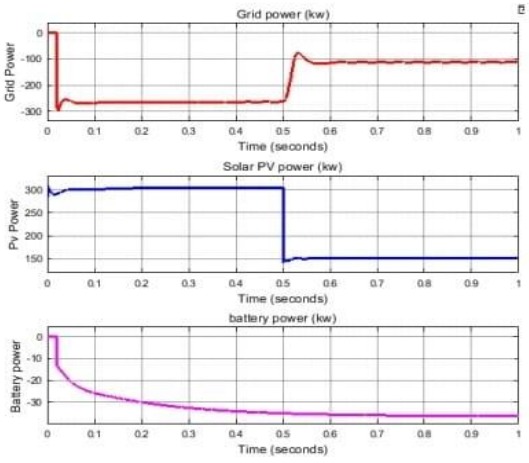

Fig. 14: Power of PV Grid and battery

The following are the battery voltage readings: 0 to 0.5 s, 258.5 to 1 s, 1 to 1.5 s, 258.4 to 1 s, 258.5 to 2 s, 258.3 to 2 to 2.5 s, 258.2 to 2.5 to 3 s, 258.4 to 3 to 3.5 s, 258.6 to 3.5 to 4 s, 258.2 to 4 to 4.5 s, 258.1 to 4.5 to 5 s, and 257.9 V from 5 to 5.5 volts. The values of the battery current are noted.

III. CONCLUSION

The paper's simulation findings demonstrate how well the ARONN EMS manages energy in a DC microgrid. One of the most important discoveries is that the PV system may optimize energy use by adjusting its output in response to changing irradiance levels. The battery exhibits adaptive charging and discharging, which improves the efficiency of energy management in general. The supercapacitor enhances system performance by efficiently controlling power availability and energy needs. The microgrid's electrical stability is indicated by the DC bus voltage readings. It also notes the dynamic behaviour of DC loads that vary and are constant.

The ARONN EMS exhibits notable benefits over a traditional approach, maximizing power delivery in variable circumstances and attaining greater power levels for the battery and supercapacitor. The ARONN system's higher power performance is highlighted in Fig. 21. All things considered, ARONN EMS increases the microgrid's system efficiency, resource allocation, and energy consumption.

REFERENCES

[1] C. Yin, H. Wu, F. Locment, and M. Sechilariu, ‘‘Energy management of DC microgrid based on photovoltaic combined with diesel generator and supercapacitor,’’ *Energy Convers. Manage.*, vol. 132, pp. 14–27, Jan. 2017.

[2] Y. Wang, Y. Li, Y. Cao, Y. Tan, L. He, and J. Han, ‘‘Hybrid AC/DC microgrid architecture with comprehensive control strategy for energy managementofsmartbuilding,’’*Int.J.Electr.PowerEnergySyst.*,vol.101, pp. 151–161, Oct. 2018.

[3] S. K. Ghosh, T. K. Roy, M. A. H. Pramanik, A. K. Sarkar, and M. A. Mahmud, ‘‘An energy management system-based control strategy for DC microgrids with dual energy storage systems,’’ *Energies*, vol. 13, no. 11, p. 2992, Jun. 2020.

[4] F. Ni, Z. Zheng, Q. Xie, X. Xiao, Y. Zong, and C. Huang, ‘‘Enhancing resilience of DC microgrids with model predictive control based hybrid energy storage system,’’ *Int. J. Electr. Power Energy Syst.*, vol. 128, Jun. 2021, Art. no. 106738.

[5] W. Jing, C. H. Lai, S. H. W. Wong, and M. L. D. Wong, ‘‘Batterysupercapacitor hybrid energy storage system in standalone DC microgrids: Areview,’’ *IET Renew. Power Gener.*, vol. 11, no. 4, pp. 461–469, Mar. 2017.

[6] J. Lv, X. Wang, G. Wang, and Y. Song, ‘‘Research on control strategy of isolated DC microgrid based on SOC of energy storage system,’’ *Electronics*, vol. 10, no. 7, p. 834, Mar. 2021.

[7] B. Long, T. Jeong, J. Deuk Lee, Y. Jung, and K. Chong, ‘‘Energy management of a hybrid AC–DC micro-grid based on a battery testing system,’’ *Energies*, vol. 8, no. 2, pp. 1181–1194, Feb. 2015.

[8] K. Sayed, A. M. Kassem, I. Aboelhassan, A. M. Aly, and A. G. Abo-Khalil, ‘‘Energy management and control strategy of DC microgrid including multiple energy storage systems,’’ in *Proc. 21st Int. Middle East Power Syst. Conf. (MEPCON)*, Dec. 2019, pp. 736–741.

[9] A.K.RajputandJ.S.Lather,‘‘EnergymanagementofaDCmicrogridwith hybrid energy storage system using PI and ANN based hybrid controller,’’ *Int. J. Ambient Energy*, vol. 44, no. 1, pp. 703–718, Dec. 2023.

[10] S. Ferahtia, A. Djerioui, H. Rezk, A. Chouder, A. Houari, and M. Machmoum, ‘‘Adaptive droop based control strategy for DC microgrid including multiple batteries energy storage systems,’’ *J. Energy Storage*, vol. 48, Apr. 2022, Art. no. 103983.

[11] Z. Lv, Y. Zhang, M. Yu, Y. Xia, and W. Wei, ‘‘Decentralised coordinated energy management for hybrid AC/DC microgrid by using fuzzy control strategy,’’ *IET Renew. Power Gener.*, vol. 14, no. 14, pp. 2649–2656, Oct. 2020.

[12] S. A. G. K. Abadi, S. I. Habibi, T. Khalili, and A. Bidram, ‘‘A model predictive control strategy for performance improvement of hybrid energy storage systems in DC microgrids,’’ *IEEE Access*, vol. 10, pp. 25400–25421, 2022.

[13] O. Hafsi, O. Abdelkhalek, S. Mekhilef, M. A. Soumeur, M. A. Hartani, and A. Chakar, ‘‘Integration of hydrogen technology and energy management comparison for DC-microgrid including renewable energies and energy storage system,’’ *Sustain. Energy Technol. Assessments*, vol. 52, Aug. 2022, Art. no. 102121.

[14] Y. Pu, Q. Li, W. Chen, and H. Liu, ‘‘Hierarchical energy management control for islanding DC microgrid with electric-hydrogen hybrid storage system,’’ *Int. J. Hydrogen Energy*, vol. 44, no. 11, pp. 5153–5161, Feb. 2019.

[15] P. Singh and J. S. Lather, ‘‘Power management and control of a gridindependent DC microgrid with hybrid energy storage system,’’ *Sustain. Energy Technol. Assessments*, vol. 43, Feb. 2021, Art. no. 100924.

[16] T. Wu, F. Ye, Y. Su, Y. Wang, and S. Riffat, ‘‘Coordinated control strategy of DC microgrid with hybrid energy storage system to smooth power output fluctuation,’’ *Int. J. Low-Carbon Technol.*, vol. 15, no. 1, pp. 46–54, Feb. 2020.
[17] M. S. Soliman, Y. Belkhier, N. Ullah, A. Achour, Y. M. Alharbi, A. A. Al Alahmadi, H. Abeida, and Y. S. H. Khraisat, ‘‘Supervisory energy management of a hybrid battery/PV/tidal/wind sources integrated in DCmicrogrid energy storage system,’’ *Energy Rep.*, vol. 7, pp. 7728–7740, Nov. 2021.
[18] H. Li, L. Fu, Y. Zhang, X. Gao, and Y. Lin, ‘‘SOC-based hybrid energy storage system dynamical and coordinated control for vessel DC microgrid,’’ in *Proc. IEEE Innov. Smart Grid Technol. Asia (ISGT Asia)*, May 2019, pp. 1381–1386.
[19] P. Wang, W. Wang, N. Meng, and D. Xu, ‘‘Multi-objective energy managementsystemforDCmicrogridsbasedonthemaximummembershipdegree principle,’’ *J. Modern Power Syst. Clean Energy*, vol. 6, no. 4, pp. 668–678, Jul. 2018.
[20] M. Vijayan, R. R. Udumula, T. Mahto, B. Lokeshgupta, B. S. Goud, C. N. S. Kalyan, P. K. Balachandran, C. Dhanamjayulu, S. Padmanaban, and B. Twala, ‘‘Optimal PI-controller-based hybrid energy storage system in DC microgrid,’’ *Sustainability*, vol. 14, no. 22, p. 14666, Nov. 2022.
[21] Q. Li, L. Yin, H. Yang, T. Wang, Y. Qiu, and W. Chen, ‘‘Multiobjective optimization and data-driven constraint adaptive predictive control for efficient and stable operation of PEMFC system,’’ *IEEE Trans. Ind. Electron.*, vol. 68, no. 12, pp. 12418–12429, Dec. 2021.
[22] Q. Li, P. Liu, X. Meng, G. Zhang, Y. Ai, and W. Chen, ‘‘Model prediction control-based energy management combining self-trending prediction and subset-searching algorithm for hydrogenelectric multipleunit train,’’*IEEE Trans. Transport. Electrific.*, vol. 8, no. 2, pp. 2249–2260, Jun. 2022.
[23] A. Abbasi, H. A. Khalid, H. Rehman, and A. U. Khan, ‘‘A novel dynamic load scheduling and peak shaving control scheme in community home energy management system based microgrids,’’ *IEEE Access*, vol. 11, pp. 32508–32522, 2023.
[24] R. Yao, X. Lu, H. Zhou, and J. Lai, ‘‘A novel category-specific pricing strategy for demand response in microgrids,’’ *IEEE Trans. Sustain. Energy*, vol. 13, no. 1, pp. 182–195, Jan. 2022.
[25] Q. Li, X. Xiao, Y. Pu, S. Luo, H. Liu, and W. Chen, ‘‘Hierarchical optimal scheduling method for regional integrated energy systems considering electricity-hydrogen shared energy,’’ *Appl. Energy*, vol. 349, Nov. 2023, Art. no. 121670.
[26] A. Alzahrani, M. U. Rahman, G. Hafeez, G. Rukh, S. Ali, S. Murawwat, F. Iftikhar, S. I. Haider, M. I. Khan, and A. M. Abed, ‘‘A strategy for multi-objective energy optimization in smart grid considering renewable energy and batteries energy storage system,’’ *IEEE Access*, vol. 11, pp. 33872–33886, 2023.
[27] A. F. Güven, N. Yörükeren, E. Tag-Eldin, and M. M. Samy, ‘‘Multiobjective optimization of an islanded green energy system utilizing sophisticated hybrid metaheuristic approach,’’ *IEEE Access*, vol. 11, pp. 103044–103068, 2023.
[28] M. Ali, M. A. Abdulgalil, I. Habiballah, and M. Khalid, ‘‘Optimal scheduling of isolated microgrids with hybrid renewables and energy storage systems considering demand response,’’ *IEEE Access*, vol. 11, pp. 80266–80273, 2023.
[29] S. Ahmad, M. Shafiullah, C. B. Ahmed, and M. Alowaifeer, ‘‘A review of microgrid energy management and control strategies,’’ *IEEE Access*, vol. 11, pp. 21729–21757, 2023.
[30] X. Lin and R. Zamora, ‘‘Controls of hybrid energy storage systems in microgrids: Critical review, case study and future trends,’’ *J. Energy Storage*, vol. 47, Mar. 2022, Art. no. 103884.
[31] B. Gu, C. Mao, B. Liu, D. Wang, H. Fan, J. Zhu, and Z. Sang,‘‘Optimal charge/discharge scheduling for batteries in energy router-based microgrids of prosumers via peer-to-peer trading,’’ *IEEE Trans. Sustain. Energy*, vol. 13, no. 3, pp. 1315–1328, Jul. 2022.
[32] L. Wang, Q. Cao, Z. Zhang, S. Mirjalili, and W. Zhao, ‘‘Artificial rabbits optimization: A new bio-inspired meta-heuristic algorithm for solving engineering optimization problems,’’ *Eng. Appl. Artif. Intell.*, vol. 114, Sep. 2022, Art. no. 105082.
[33] H.Abouobaida,L.deOliveira-Assis,E.P.P.Soares-Ramos,H.Mahmoudi, J. M. Guerrero, and M. Jamil, ‘‘Energy management and control strategy of DC microgrid based hybrid storage system,’’ *Simul. Model. Pract. Theory*, vol. 124, Apr. 2023, Art. no. 102726.